

See discussions, stats, and author profiles for this publication at: <https://www.researchgate.net/publication/24236257>

Absolute Quantification of Potential Cancer Markers in Clinical Tissue Homogenates Using Multiple Reaction Monitoring on a Hybrid Triple Quadrupole/Linear Ion Trap Tandem Mass Spec...

ARTICLE in ANALYTICAL CHEMISTRY · APRIL 2009

Impact Factor: 5.64 · DOI: 10.1021/ac802726a · Source: PubMed

CITATIONS

59

READS

42

4 AUTHORS, INCLUDING:



Leroi V Desouza

SCIEX

57 PUBLICATIONS 1,799 CITATIONS

SEE PROFILE



Alex Romaschin

University of Toronto

121 PUBLICATIONS 3,477 CITATIONS

SEE PROFILE

Absolute Quantification of Potential Cancer Markers in Clinical Tissue Homogenates Using Multiple Reaction Monitoring on a Hybrid Triple Quadrupole/Linear Ion Trap Tandem Mass Spectrometer

Leroi V. DeSouza,[†] Alexander D. Romaschin,^{‡,§} Terence J. Colgan,^{§,||} and K. W. Michael Siu^{*†}

Department of Chemistry and Centre for Research in Mass Spectrometry, York University, 4700 Keele Street, Toronto, Ontario, Canada M3J 1P3, Division of Clinical Biochemistry, St. Michael's Hospital, 30 Bond Street, Toronto, Ontario, Canada M5B 1W8, Department of Laboratory Medicine and Pathobiology, University of Toronto, Toronto, Ontario, Canada M5G 1L5, and Pathology and Laboratory Medicine, Mount Sinai Hospital, 600 University Avenue, Toronto, Ontario, Canada M5G 1X5

Multidimensional liquid chromatography with tandem mass spectrometry with iTRAQ-labeling typically used for differential expression analysis in biomarker discovery does not always detect peptides from these biomarkers in all samples analyzed. Herein we describe the results of targeted analyses using multiple reaction monitoring (MRM) on a hybrid triple quadrupole/linear ion-trap tandem mass spectrometer. The MRM approach when combined with the newly released mTRAQ reagent, a non-isobaric variant of the iTRAQ tag available in two versions, enables absolute quantification of peptides and proteins via isotope-dilution mass spectrometry. This approach was applied to clinical endometrial tissue homogenates in an effort to quantify two endometrial cancer biomarkers, pyruvate kinase (PK) and polymeric immunoglobulin receptor (PIGR). We successfully demonstrated the feasibility of this approach on 20 individual samples and further verified the differential expressions of these two biomarkers in endometrial carcinoma. PK was determined to be present at an average concentration of 58.33 pmol/mg of total proteins and in the range of 9.13–87.66 pmol/mg in the soluble fraction of the normal proliferative endometrium homogenates. By contrast, the average concentration of PK in the cancer sample homogenates was 237.2 pmol/mg of total proteins and in the range of 66.10–570.9 pmol/mg. PIGR was found to be expressed at an average concentration of 8.85 pmol/mg of total proteins with a range of 1.02–49.61 pmol/mg in the normal proliferative control samples, and an average concentration of 200.2 pmol/mg with a range of 7.63–810.4 pmol/mg in the cancer samples. This study confirmed qualitatively the differential expressions previously observed but also showed that the actual relative differential expressions in these samples were much higher than those reported in the discovery study. These results validated earlier observations of dynamic-range compression in iTRAQ-labeling with hybrid quadrupole/time-of-flight mass spectrometry (DeSouza, L.V. et al. *J. Proteome Res.* 2008, 7, 3525–3534).

Over the past few years, there has been a marked increase of biomarker research activities. This surge in interest is, in large

part, a result of the development of newer labeling techniques that have enabled relative quantification to evolve from conventional two-dimensional gel-based approaches, including Differential In Gel Electrophoresis (DIGE), to mass spectrometry. We have previously employed some of these techniques, namely ICAT¹ and iTRAQ² mass-tagging, with considerable success in our investigations into endometrial, head-and-neck, glioblastoma multiforme, and renal cancers.^{3–7} In particular, the iTRAQ approach has resulted in the discovery of a number of potential markers for these cancers; some of these biomarkers were verified by independent techniques on additional cohorts of samples.^{6,8,9} The iTRAQ approach was particularly well-suited for our discovery studies, as the labels were available in four versions that permitted simultaneous comparisons between a control and three other patient samples. There were, however, two issues with this technology that required attention. The first was that the iTRAQ approach provided quantification only relative to the control used in each group. Second, proteins of interest, particularly those present at relatively low abundances, were not always detected and quantified. This second issue can be addressed by using a strategy where peptides from the proteins of interest are targeted for analysis. Such targeted analysis is typically achieved using the multiple reaction monitoring (MRM) mode on a triple-quadrupole-

- (1) Gygi, S. P.; Rist, B.; Gerber, S. A.; Turecek, F.; Gelb, M. H.; Aebersold, R. *Nat. Biotechnol.* 1999, 17, 994–999.
- (2) Ross, P. L.; Huang, Y. N.; Marchese, J. N.; Williamson, B.; Parker, K.; Hattan, S.; Khainovski, N.; Pillai, S.; Dey, S.; Daniels, S.; Purkayastha, S.; Juhasz, P.; Martin, S.; Bartlett-Jones, M.; He, F.; Jacobson, A.; Pappin, D. J. *Mol. Cell. Proteomics* 2004, 3, 1154–1169.
- (3) DeSouza, L.; Diehl, G.; Yang, E. C.; Guo, J.; Rodrigues, M. J.; Romaschin, A. D.; Colgan, T. J.; Siu, K. W. M. *Proteomics* 2005, 5, 270–281.
- (4) DeSouza, L.; Diehl, G.; Rodrigues, M. J.; Guo, J.; Romaschin, A. D.; Colgan, T. J.; Siu, K. W. M. *J. Proteome Res.* 2005, 4, 377–386.
- (5) DeSouza, L. V.; Grigull, J.; Ghanny, S.; Dubé, V.; Romaschin, A. D.; Colgan, T. J.; Siu, K. W. M. *Mol. Cell. Proteomics* 2007, 6, 1170–1182.
- (6) Ralhan, R.; Desouza, L. V.; Matta, A.; Chandra Tripathi, S.; Ghanny, S.; Datta Gupta, S.; Bahadur, S.; Siu, K. W. M. *Mol. Cell. Proteomics* 2008, 7, 1162–1173.
- (7) Siu, K. W. M.; DeSouza, L. V.; Scorilas, A.; Romaschin, A. D.; Honey, R. J.; Stewart, R.; Pace, K.; Youssef, Y.; Chow, T. F. F.; Youssef, G. M. *J. Proteome Res.* accepted September 5, 2008.
- (8) Dubé, V.; Grigull, J.; DeSouza, L. V.; Ghanny, S.; Colgan, T. J.; Romaschin, A. D.; Siu, K. W. M. *J. Proteome Res.* 2007, 6, 2648–2655.
- (9) Matta, A.; DeSouza, L. V.; Shukla, N. K.; Gupta, S. D.; Ralhan, R.; Siu, K. W. M. *J. Proteome Res.* 2008, 7, 2078–2087.

* To whom correspondence should be addressed. E-mail: kwmsiu@yorku.ca.
Phone: (416)650-8021. Fax: (416)736-5936.

[†] York University.

[‡] St. Michael's Hospital.

[§] University of Toronto.

^{||} Mount Sinai Hospital.

type mass spectrometer. Under MRM, the mass spectrometer is set up to monitor only specific mass/charge (m/z) values of interest; as a consequence, the probability of detecting even low levels of a peptide in the presence of a complex mixture of peptides is much higher. MRM has been the method of choice for quantification of low levels of small molecules, including drugs or metabolites, as well as peptides.^{10–13} In brief, the first quadrupole, Q1, is set to transmit ions matching the m/z value of a multiply protonated peptide of interest; these ions are then fragmented in q2 by collision-induced dissociation (CID). In turn, Q3 is set to transmit only those product ions of a particular m/z value deemed to be diagnostic for the peptide monitored. This combination of the Q1 and Q3 m/z values is referred to as an MRM transition. The acquisition method is typically set up to cycle through a series of such transitions each lasting a time of milliseconds, thereby affording sequential monitoring of many peptides of interest. This near simultaneous detection of multiple dissociations of a particular peptide serves to increase confidence in the peptide's identification and quantification.

Overcoming the (first) issue on limitations to relative quantification requires the use of specific peptides as quantification standards which are isotopically different from the patient samples. This can be accomplished by either incorporating specific isotopes during peptide synthesis or labeling the specific peptide with custom-designed mass-tags. We have recently described the application of such mass-tagging reagents, mTRAQ (Applied Biosystems, Foster City, CA) for absolute quantification of targeted biomarkers in endometrial cancer (EmCa) tissue homogenates.¹⁴ As previously described the mTRAQ tags, while chemically identical to those of iTRAQ, differ in their isotopic contents.¹⁴ Specifically, the mTRAQ reagent is available in two versions: the "heavy" version is identical to the iTRAQ 117 tag; the "light" version is devoid of any intentional isotopic enrichment.¹⁴ Consequently, the light version has a monoisotopic mass of 141 Da versus 145 Da of that in the heavy version. By virtue of this mass difference, unique MRM transitions can now be generated for any given peptide that is labeled with the mTRAQ tags.¹⁴ In turn, this means that in a sample mixture where peptides originating from different sources are tagged separately with the heavy and light labels, the two versions can be monitored independently and distinctly. By contrast, the iTRAQ tags being isobaric lack this level of specificity. Quantification in MRM via isotope-dilution mass spectrometry offers the most accurate methodology for specific assaying of analytes in complex matrices that require multiple purification steps prior to mass spectrometric analysis.¹⁵

In our preliminary study with mTRAQ, we investigated the feasibility of this approach by quantifying one potential biomarker in selected endometrial tissue homogenate samples.¹⁴ In this study, we have chosen to focus on the absolute quantification of two potential endometrial cancer biomarkers that we had previ-

ously discovered using the iTRAQ approach in a larger cohort of samples. Described herein are the results of this expanded study where the same biomarker, pyruvate kinase (PK) M1/M2, as well as a second biomarker, polymeric immunoglobulin receptor (PIGR), were quantified in 20 human endometrial tissue homogenates. These 20 samples were a subset of those used in our discovery-phase study⁵ and were composed of 10 normal endometrial samples in the proliferative phase of the menstrual cycle and 10 type I endometrial cancer samples. Our reasons for focusing on PK have previously been detailed,¹⁴ but briefly, PK is an enzyme playing a key role in the glycolytic pathway, where it catalyzes the conversion of phosphoenol pyruvate (PEP) to pyruvate and generates ATP from ADP in the process. PK expresses as a number of isoforms, with M1 and M2 being splice variants of a single gene; the difference between the two isoforms is located in exons 9 and 10, which encode a stretch of 56 residues that have differences in 22 positions.^{16,17} The M1 isoform is expressed in skeletal muscle and brain tissue, while the M2 isoform is found in fetal tissue and proliferating cells, including adult stem cells, early embryonic cells, and cancer cells.^{16–18} As ATP production by PK is independent of oxygen levels, it was initially suggested that the enzyme plays a role in the survival of cells under the hypoxic conditions typically prevalent in tumors.¹⁶ That view has more recently been challenged by studies suggesting PK-M2 negatively regulates the production of ATP so as to provide glycolytic intermediates that are vital for the syntheses of cell components.¹⁶ This apparent paradox can perhaps at least partially be explained by the fact that PK-M2 found in normal proliferating cells is present in a highly active tetrameric form, while that found in tumors is an almost inactive dimeric form.¹⁶ As this dimeric form is prevalent only in tumors, it is also often referred to as tumor PK-M2.

Our other protein of interest, PIGR, was also identified as a potential cancer biomarker for endometrial cancer using both cICAT as well as iTRAQ labeling.^{4,5} Differential expression, particularly in type I endometrial cancer, was also verified using Western blot analysis.⁵ Notably, whereas differential expression was observed in almost all cancer samples for PK-M2, this was not always the case for PIGR. The majority of the endometrial cancer type I samples displayed differential expression relative to the normal controls; however, four out of the twelve type I cancer samples showed no significant difference in expression levels, and the experiments failed to detect PIGR in two of the samples.⁵ PIGR is part of the humoral immune response and is expressed in epithelial cells. Its primary role is believed to be the transport of dimeric IgA, and to a lesser extent IgM, from the basolateral surface to the apical surface of the epithelial cells where it is released into the exocrine secretions.¹⁹ At the apical surface, the extracellular ligand-binding portion of PIGR is cleaved, resulting in either free PIGR or its complex with IgA. This cleaved portion of PIGR is also known as the secretory component (SC).¹⁹ We proposed that one possible reason for increase in the

(10) Finlay, E. M.; Games, D. E.; Startin, J. R.; Gilbert, J. *Biomed. Environ. Mass Spectrom.* **1986**, *13*, 633–639.

(11) Phillips, W. H., Jr.; Ota, K.; Wade, N. A. *J. Anal. Toxicol.* **1989**, *13*, 349–355.

(12) Anderson, L.; Hunter, C. L. *Mol. Cell. Proteomics* **2006**, *5*, 573–588.

(13) Luna, L. G.; Williams, T. L.; Pirkle, J. L.; Barr, J. R. *Anal. Chem.* **2008**, *80*, 2688–2693.

(14) DeSouza, L. V.; Taylor, A. M.; Li, W.; Minkoff, M. S.; Romaschin, A. D.; Colgan, T. J.; Siu, K. W. M. *J. Proteome Res.* **2008**, *7*, 3525–3534.

(15) Siu, K. W. M.; Bednas, M. E.; Berman, S. S. *Anal. Chem.* **1983**, *55*, 473–476.

(16) Mazurek, S.; Boschek, C. B.; Hugo, F.; Eigenbrodt, E. *Semin. Cancer Biol.* **2005**, *15*, 300–308.

(17) Ugurel, S.; Bell, N.; Sucker, A.; Zimpfer, A.; Rittgen, W.; Schadendorf, D. *Int. J. Cancer* **2005**, *117*, 825–830.

(18) Christofk, H. R.; Vander Heiden, M. G.; Harris, M. H.; Ramanathan, A.; Gerszten, R. E.; Wei, R.; Fleming, M. D.; Schreiber, S. L.; Cantley, L. C. *Nature* **2008**, *452*, 230–233.

(19) Kaetzel, C. S. *Immunol. Rev.* **2005**, *206*, 83–99.

expression level of PIGR in endometrial cancer type I samples may be a consequence of the host response to the presence of the cancerous cells or to the carcinogenic stimuli; additionally, we further hypothesized that this may, in fact, be one reason for the less aggressive nature of the type I cancer relative to type II.⁵ This view has recently been espoused by others who noted that PIGR expression level correlates with certain forms of gastric cancer.²⁰ In this later study, 57.7% of the gastric adenocarcinomas expressing PIGR exhibited the presence of metastatic adenocarcinomas in the lymph nodes; this percentage, however, escalated to 93.7% for those adenocarcinomas that did not express PIGR.²⁰ These results led the authors of that study to independently speculate that “PIGR may function to increase the local humoral immunity in the tumor and that, in cases with lower PIGR expression, changes in IgA-related immune response in the tumor environment may lead to increased metastatic potential of the tumor cells”, an opinion that is in keeping with our earlier hypothesis.

EXPERIMENTAL SECTION

Sample Preparation. As described above, most of the tissue homogenates used in this study were aliquots of those used in the discovery phase that had been archived at -80°C .⁵ There was only one sample used here that had not been used in the previous study. This sample was used in place of a normal proliferative sample that had been exhausted. Patient consent and tissue-banking procedures were approved by the research ethics boards of York University, Mount Sinai Hospital, University Health Network, and North York General Hospital. All samples were processed as follows: resected tissue that had been flash-frozen within 20 min of devitalization was sectioned and classified by a pathologist (TJC). The mirror face of the section used for classification, typically a few cubic mm, was washed three times in 1.0 mL of cold phosphate-buffered saline (PBS) at 4°C and then homogenized in 0.5 mL of cold PBS with a cocktail of protease inhibitors (1 mM AEBSF (4-(2-aminoethyl) benzene-sulfonyl fluoride), 10 μM leupeptin, 1 $\mu\text{g}/\text{mL}$ aprotinin, and 1 μM pepstatin) at 30,000 rpm using a Polytron PT 1300D hand-held homogenizer (Brinkmann, Westbury, U.S.A.). The homogenate was then centrifuged for 30 min in a microfuge at 4°C , and the supernatant transferred to a fresh tube and stored at -80°C until further analysis.

Synthetic Peptides. Three peptides were chosen for this study: two were specific for PK M1/M2, while a third was for PIGR. The two peptides for pyruvate kinase were PK1 (GVNLP-GAAVDLPVSEK) and PK2 (LDIDSPPTAR), while that for PIGR was designated PIGR1 (VYTVDLGR), which maps to the SC portion of PIGR. Both PK peptides employed were from regions common to both M1 and M2 isoforms. These peptides were custom-synthesized by Sigma Genosys, TX, at stated purities of $\geq 95\%$, 85%, and 95%, respectively. Each peptide received was initially dissolved in distilled water at a nominal concentration of 10 mM. These peptide stock solutions were sent for independent purity analyses to determine the amino acid content (by amino acid analysis) and the proportion of the specific peptide therein; the latter was quantified by direct infusion-MS analysis of the

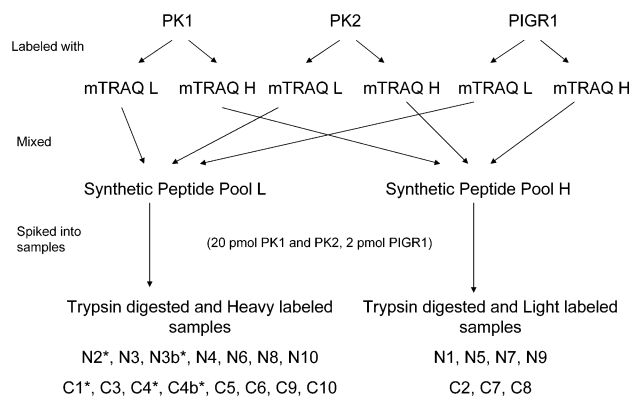


Figure 1. Flowchart of experimental set up. Each labeled synthetic peptide pool containing 20 pmol of PK1 and PK2, and 2 pmol of PIGR1 was spiked into oppositely labeled samples containing 100 μg of total protein with the exception of those that are indicated by an asterisk, where only 75 μg of total protein was used.

desalted sample, and estimating the area of the expected mass peak relative to the total area of all peaks observed. The following results were returned: PK1, 91.2 and 91%; PK2, 86.8 and 86%; and PIGR1, 76.8 and 79%, respectively. These numbers were then used to calculate the actual concentrations of the peptides in the samples.

Mass Tagging. Approximately 10 nmol of each of the synthetic peptide was labeled with an mTRAQ reagent for the isotope-dilution experiment. Labeling of the synthetic peptides was performed in duplicate with one each of the heavy and light versions of the mTRAQ reagents, while an approximately 100 μg aliquot of the tryptic digest of each tissue homogenate was labeled with either of the versions of mTRAQ reagent. As described earlier, labeling efficiency of the synthetic peptides were checked by targeting the expected m/z ratios of the unlabeled versions of the peptide in combination with the most intense fragment ions. For PK1 and PK2, the efficiencies were better than 99%,¹⁴ while that for PIGR1 was 96% and 94% for the light and heavy label, respectively (Supporting Information, Figure S1). Trypsin digestion and labeling were performed as previously described.^{4,5,14} Aliquots of the labeled PK1, PK2, and PIGR1 quantification standards were combined to form a pool of like-labeled reference peptides; 20 μL of which was then mixed with the 100 μL of the oppositely labeled homogenate solutions to give analytical samples with approximately, but accurately known, 20 pmol of PK peptides and 2 pmol of PIGR1 (Figure 1). The mixtures were then speed-vacuumed to dryness before being redissolved in a final volume of 1 mL of Strong Cation Exchange (SCX) Eluent A (see below). On the basis of the aforementioned peptide purities, the working concentrations of the labeled peptide pools that had been spiked at nominal quantities of 20 pmol in the case of each PK peptide were actually 16.6 pmol (PK1) and 14.9 pmol (PK2), and the 2 pmol nominal quantity for PIGR1 was actually 1.2 pmol. The spike amounts had been empirically determined in our preliminary study with PK as well as subsequent test runs for PIGR as being optimal for these samples as their actual concentrations tended to be in this range.¹⁴

As alluded to above, each tissue-homogenate sample was randomly labeled with either a heavy or a light mTRAQ reagent to eliminate any bias introduced as a result of differences in labeling efficiency between the two mTRAQ tags. Of the 20

(20) Gologan, A.; Acquafondata, M.; Dhir, R.; Sepulveda, A. R. *Arch. Pathol. Lab. Med.* **2008**, *132*, 1295–1301.

samples, N1, N5, N7, N9, C2, C7, and C8 ("N" being normal proliferative samples and "C" EmCa samples) were labeled with the light version, while the rest were labeled with the heavy version (Figure 1). For each sample, we typically worked with 100 μg of total proteins, the same amount used in the discovery phase;⁵ however, for three samples (N2, C1, and C4) we had to use approximately 75 μg , because of sample availability. To verify that the results obtained using 75 μg aliquots did not significantly differ from those obtained with 100 μg aliquots (as a result of reduced signal-to-noise), two aliquots of one sample (N3) were prepared, one with 75 μg (71.85 μg by subsequent confirmatory Bradford assay; N3b) and the second with 100 μg (N3, confirmed to be accurate by Bradford assay) of total protein to which the same amounts of quantification standards were added. In addition, to corroborate the results obtained for this set of samples with those from the preliminary analysis, we also compared the results for one cancer sample (C4) obtained with quantification standard solutions prepared for experiments in this study with those obtained with the same sample using standard solutions used in the previous analysis (C4b).¹⁴ In both these cases, we used approximately 75 μg total protein. Of the 23 samples described in this study, all except N2, N3b, C1, C4, and C4b, were processed at the same time. The five exceptions listed were processed as a group on a separate day.

Strong Cation Exchange Separation. After mixing, the resulting samples were vacuum-centrifuged to dryness and redissolved in SCX Eluent A (1.0 mL of 10 mM KH_2PO_4 in 25% acetonitrile, adjusted with phosphoric acid to pH 3.0). Each of these samples was then fractionated by manual injection onto a 0.2 mL capacity SCX cartridge supplied as part of an ICAT kit (Applied Biosystems, Foster City, CA) followed by a wash with 1.0 mL of Eluent A and step-elutions using 0.5 mL each of Eluent A with increasing concentrations of KCl. As the three peptides of interest eluted in the 100 mM KCl fraction in test runs, the salt concentrations used were 50 mM, 100 mM, 150 mM, and 1 M KCl, with the 100 mM salt fraction being the only one analyzed for the remainder of the study. This fraction from each of the samples was vacuum-centrifuged to dryness and redissolved in 30 μL of 1.0% formic acid.

Reverse-Phase nanoLC-MS/MS Analysis. Reverse-phase (RP) nanoLC separation was performed with a Tempo nano MDLC system with autosampler (Applied Biosystems/MDS SCIEX) coupled online with a QTRAP 4000 hybrid triple quadrupole/linear ion trap mass spectrometer (Applied Biosystems/MDS SCIEX). One-tenth of the redissolved 100 mM eluate fraction was loaded on to a 5 μm particle, 5 mm length \times 300 μm ID, 100 Å pore size, RP-C18 trapping cartridge (LC Packings, Amsterdam, The Netherlands) fitted onto a switching valve (VICI, Houston, TX). The sample was loaded and desalted using an aqueous solution of 5% acetonitrile in 0.1% formic acid (Solvent A). Desalting was performed at a flow rate of 20 $\mu\text{L}/\text{min}$ for 5 min before the precolumn was switched in-line with the analytical column (150 mm length \times 75 μm ID, packed in-house with 3 μm , 100 Å pore, Kromasil beads). Peptides were eluted using a nonlinear binary gradient of Solvent A (0.1% formic acid in 5% acetonitrile) and Solvent B (0.1% formic acid in 95% acetonitrile) as described below at a flow rate of 200 nL/min. Each sample was injected a minimum of two times with blank runs performed between each injection

Table 1. MRM Transitions Used^a

peptide	label type	charge state	Q1 mass (m/z)	Q3 masses (m/z)	CE used
PK1	Light	2+	959.3	524.2 (b4)	51.70
				883.3 (y7)	
		3+	639.7	770.6 (y6)	37.60
	Heavy	2+	963.3	524.5 (b4)	51.70
				528.1 (b4)	
		3+	642.2	887.1 (y7)	37.60
PK2	Light	2+	669.4	774.4 (y6)	38.96
				824.4 (b8)	
		3+	446.6	528.5 (b4)	29.18
	Heavy	2+	671.4	741.4 (y7)	38.96
				601.4 (b4)	
		3+	447.9	688.5 (b5)	29.18
PIGR1	Light	2+	531.8	557.4 (y5)	32.90
				601.4 (b4)	
		3+	533.8	718.6 (b5)	32.90
	Heavy	2+	533.8	823.5 (y7)	32.90
				345.3 (y3)	
		3+	533.8	722.6 (b5)	32.90

^a The specific product ions that matched the m/z ratios selected in Q3 are indicated within parentheses. The collision energy (CE) used for each precursor mass is shown in the last column, this CE was determined based on the CE used in test runs for each of these peptides under the same LC-MS run conditions.

to prevent any possible carryover between runs. All 23 samples were run once prior to beginning the second set of injections.

time (min)	0	10	20	50	58	70	72	89
% B	5	5	30	65	80	80	5	5

MRM Transitions. Preliminary tests using the labeled synthetic peptides were run with an acquisition method that included an enhanced MS scan followed by enhanced product ion (EPI) scans with a rolling collision energy (data not shown). These scans provided information on the charge states of the peptide ions as well as the most-prominent fragment ions detected under the run and collision-energy conditions. A second acquisition method which included an MRM scan based on these expected precursor and product ions m/z ratios, followed by two EPI scans at a scan rate of 1000 Da/s that were triggered by a positive detection of the specific MRM transition event was then developed and used in the analysis of the actual samples. Dwell times for all transitions were set at 29 ms. As the EPI scans in this method were used merely for purposes of verifying the peptide identity, and as the peak widths (full width at half-height) were typically 20–30 s, the dynamic exclusion in the method was set to exclude the precursor ion for a period of 60 s after the initial EPI scan. MRM transition data were acquired using unit-resolution settings for both Q1 and Q3 to minimize any possibility of contribution from the oppositely labeled peptide. The transitions used to detect the three peptides of interest are listed in Table 1. One example of the MRM traces obtained for each peptide (both labels) being monitored is shown

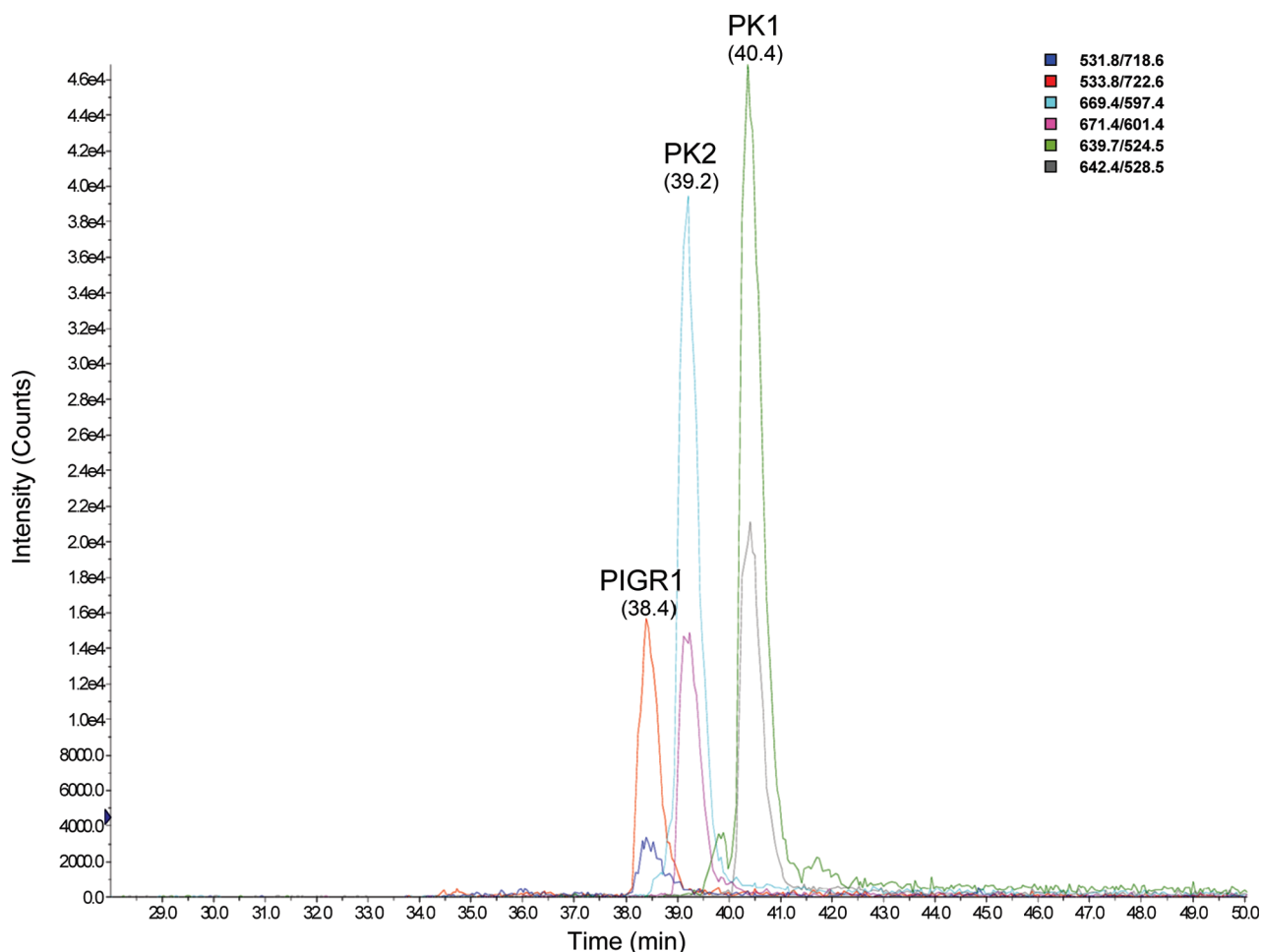


Figure 2. Representative MRM traces (taken from N4 Run 3) for each mTRAQ-labeled peptide. PK1: 639.7/524.5 (L), 642.2/528.5 (H); PK2: 669.4/597.4 (L), 671.4/601.4 (H); PIGR1: 531.8/718.6 (L), 533.8/722.6 (H).

in Figure 2. Abundances were calculated on the basis of the peak area after integration, using the IntelliQuan algorithm provided in the Analyst 1.4.1 software. As each MRM peak (baseline to baseline) was in the range of 1 min wide and the transitions were monitored on the tens of millisecond time scale with a maximum of 100 transitions possible, each MRM peak was typically composed of 20 data points or more. Only peaks with areas $\geq 10,000$ counts were considered in the calculation. As listed in Table 1, each peptide was monitored using multiple transitions and, in some cases, different charge states. Individual ratios for each pair of transitions whose abundances exceeded the specified cutoff were averaged to yield the reported ratio for the particular peptide in a given run (see Supporting Information, Figure S2). Ratios for the peptide from multiple runs were again averaged and normalized so as to be expressed relative to light-labeled reference peptides, and these are shown in Table 2.

RESULTS AND DISCUSSION

The results of the quantification of PK and PIGR are summarized in Table 2. As mentioned in the Experimental Section, the ratios reported for each peptide are averages of the individual ratios obtained for each pair of MRM transitions, provided that the areas under the respective curves were both above the threshold cutoff of 10,000 counts (see Supporting Information, Table S1 and Figure S2). The threshold was empirically determined in a preliminary study to provide reliable data.¹⁴ As evident

in the Supporting Information, Figure S2, transitions with peak areas below the cutoff are typically from peaks that are indistinguishable from background noise. All ratios are expressed as MRM peak areas from the endogenous peptide relative to that from the reference peptide. The run-to-run variation in ratios for each of the peptides in the 23 samples run was very good with a coefficient of variation (CV) ranging from 0.03% to 23.3% with one outlier at 49.5% and a median value of 5.8% (Table 2). As the quantification for some samples was performed relative to a light-labeled peptide reference pool while others were relative to the heavy-labeled pool, the ratios of samples that were quantified relative to the heavy labeled pool were normalized by multiplying the raw data with the relative ratio obtained for the individual peptide in the 1:1 comparison of the heavy and light labeled pools (Table 2; sample S1). This normalized ratio was used to calculate the absolute abundance of the peptide in each case. The absolute amount of PK was then calculated as the average of the absolute amounts of PK1 and PK2. Encouragingly, in most cases, the quantification by PK1 and PK2 individually is comparable, with CVs between the two absolute values across all 22 samples ranging from 0.28% to 23.8% with one at outlier 47.2% and a median value of 9.5%. The single outlier was for sample N8. This, however, is not surprising as the intensity of the endogenous peptides were weak and their abundances relative to those of the reference peptides in that sample were in excess of an order of magnitude

Table 2. Determination of Protein Concentrations^a

sample	peptide	average ratio (CV %)	number of runs averaged	conc. pmol/mg	final protein conc. pmol/mg (CV %)
N1	PK1	0.33 (15.0)	2	54.75	61.06 (14.6)
	PK2	0.45 (19.7)	3	67.38	
	PIGR1	0.19	1	2.32	
N2	PK1	0.22 (10.1)	3	48.20	44.98 (10.1)
	PK2	0.21 (1.8)	3	41.75	
	PIGR1	0.12 (14.1)	3	1.86	
N3	PK1	0.31 (0.0)	2	51.98	54.76 (7.2)
	PK2	0.39 (2.4)	2	57.53	
	PIGR1	0.28	1	3.37	
N4	PK1	0.34 (1.8)	2	56.12	63.90 (17.2)
	PK2	0.48 (9.0)	3	71.68	
	PIGR1	4.09 (18.7)	2	49.61	
N5	PK1	0.44 (8.9)	3	73.62	78.99 (9.6)
	PK2	0.57 (22.9)	3	84.37	
	PIGR1	0.35	1	4.21	
N6	PK1	0.38 (2.5)	2	62.54	62.66 (0.3)
	PK2	0.42 (0.7)	2	62.79	
	PIGR1	0.37 (0.7)	2	4.50	
N7	PK1	0.37 (2.8)	2	61.99	63.00 (2.3)
	PK2	0.43 (5.0)	2	64.00	
	PIGR1	0.25 (23.3)	2	2.99	
N8	PK1	0.04	1	6.08	9.13 (47.2)
	PK2	0.08 (8.5)	2	12.18	
	PIGR1	0.08	1	1.02	
N9	PK1	0.57 (10.9)	2	94.58	87.66 (11.2)
	PK2	0.54 (13.0)	2	80.73	
	PIGR1	0.23	1	2.84	
N10	PK1	0.34 (8.1)	2	56.80	57.13(0.8)
	PK2	0.38 (0.4)	2	57.45	
	PIGR1	1.28	1	15.50	
C1	PK1	2.87 (3.5)	3	635.6	570.9 (16.0)
	PK2	2.54 (1.0)	3	506.2	
	PIGR1	35.15 (10.2)	3	568.6	
C2	PK1	2.60 (6.0)	2	431.5	370.6 (23.2)
	PK2	2.07 (9.1)	2	309.7	
	PIGR1	32.72 (5.1)	2	397.1	
C3	PK1	1.34 (3.2)	2	222.9	198.3 (17.6)
	PK2	1.16 (9.6)	2	173.6	
	PIGR1	6.86 (14.5)	2	83.22	
C4	PK1	1.00 (8.1)	3	220.6	219.8 (0.5)
	PK2	1.10 (3.8)	3	219.1	
	PIGR1	3.32 (7.4)	3	53.62	
C5	PK1	1.14 (9.8)	2	189.0	188.5 (0.3)
	PK2	1.26 (3.9)	3	188.1	
	PIGR1	1.95 (6.5)	2	23.66	
C6	PK1	1.43 (2.0)	2	237.9	251.9 (7.8)
	PK2	1.78 (8.4)	3	265.8	
	PIGR1	1.61 (2.9)	2	19.54	
C7	PK1	0.37 (13.1)	2	61.39	66.12 (10.1)
	PK2	0.47 (1.8)	2	70.84	
	PIGR1	66.79 (13.2)	2	810.4	
C8	PK1	0.94 (1.0)	2	156.6	146.8 (9.4)
	PK2	0.92 (3.6)	2	137.0	
	PIGR1	0.63	1	7.63	
C9	PK1	1.23 (8.6)	2	203.6	200.4 (2.3)
	PK2	1.32 (0.3)	2	197.2	
	PIGR1	0.75 (2.9)	2	9.05	
C10	PK1	0.79 (6.6)	2	131.9	158.6 (23.8)
	PK2	1.24 (5.3)	3	185.2	
	PIGR1	2.42 (4.3)	2	29.40	
N3b	PK1	0.21 (13.4)	3	48.80	47.19 (4.8)
	PK2	0.22 (2.6)	3	45.57	
	PIGR1	0.23 (49.4)	3	3.89	
C4b	PK1	0.96 (8.2)	3	211.6	201.1 (7.4)
	PK2	0.96 (0.1)	3	190.6	
	PIGR1	1.00 (14.7)	4		
S1	PK1	1.19 (2.7)	4		
	PK2	1.19 (2.7)	4		
	PIGR1	1.29 (5.6)	4		

^a Each peptide ratio is calculated based on the average of all the different monitored transitions that exceed the cutoff threshold specified. The average ratio reported in each case was averaged across up to four runs with the corresponding CV shown in parentheses with the exception of those where the particular peptide was only quantified in a single run, in which case a CV could not be calculated. The average ratio is expressed relative to the light-labeled reference peptide; samples that were initially mixed with the heavy-labeled reference pool were, therefore, normalized accordingly using the ratios of the reference peptides listed in S1. Concentrations were calculated as follows: (average ratio × nominal peptide conc × peptide purity × 1000) / sample total protein concentration in (μg). Peptide purity was calculated as the product of the amino-acid purity and the proportion of the actual peptide within the synthetic peptide solution as analyzed. The final protein concentration for PK was the average of the concentrations as determined by PK1 and PK2, while that for PIGR was the concentration as determined by PIGR1.

with PK1 being present at 1/25th of the reference peptide intensity. Triplicate injections of mixtures of heavy and light mTRAQ-labeled peptides spiked at different relative amounts up to an order of magnitude difference between the two labeled

versions of the peptides (in both directions) determined the range of quantification using mTRAQ, to be linear with coefficients of determination (r^2) better than 0.99 (data not shown). We expect that the CV for N8 would have been considerably less, if we

had used a diluted reference peptide pool that was more comparable with the endogenous expression level. This would, however, require multiple levels of spiking and was deemed to be excessive in the current experiments. Nevertheless, this serves to illustrate the importance of ensuring that the reference peptide amount is within the approximate range of the endogenous peptides for proper quantification. As discussed in our previous study, the CV in the quantification by the two peptides might further be improved with a different choice of a reference peptide. In this instance, in the full length protein, PK1 was immediately preceded by two tandem lysine residues which could lead to a missed cleavage after the second lysine that would in turn lead to an underestimation in the absolute amount of PK1.¹⁴

Ideally, multiple reference peptides for each protein would improve the quantification; however, as noted in the case of PIGR, we have only used one peptide for quantification. This is because the second peptide intended for use in this study, although detected frequently in the discovery phase, did not solubilize properly when synthesized as a peptide (or at least the synthetic peptide had poor solubility). We, therefore, resorted to using a single peptide for quantifying PIGR. Mindful of this, the quantification of PIGR should be regarded as less reliable than that of PK-M2. This is particularly relevant in the cases of samples C1, C2, and C7 where the relative intensities were all more than 25 fold higher than the reference peptide standard. Again, in these cases, a more accurate determination of the expression levels would have been obtained using multiple reference standard concentrations. However, this would have increased the number of required analyses beyond the scope of this study. To ensure that the number of analyses was still manageable, we adopted the common strategy in isotope dilution in employing a single concentration of reference standard that was a compromise of the expected protein levels for all samples.

The reproducibility of this mTRAQ approach was demonstrated by the analysis across different preparations and conditions for the same sample as determined by the comparisons between N3 and N3b, as well as C4 and C4b, which show similar CVs. The CV in the total protein concentrations reported for the first pair of samples, where different amounts of starting tissue homogenate were used, was 10.5% for PK and 10.2% for PIGR, while that of the second pair where the current reference pool mix was compared with results using the reference pool from the previous study was 6.3% for PK.

We also compared the amount of PIGR determined in these samples with the Western blot analysis results we had previously reported for these same samples.⁵ In Figure 3, the samples are rearranged so as to pair up in the same order as that used in the previous iTRAQ study and Western analysis. As shown therein, the absolute amounts of PIGR reflect the trends in spot intensities in the Western dot blot analysis in general. This trend is even stronger when one accounts for the discrepancies in loading amounts, as is evident from the actin loading control intensities. In fact, as evident from this figure, the relative amounts of the three samples with the highest concentrations of PIGR (as determined by this mTRAQ study), in comparison with that of the normal control samples with which they were originally grouped in the iTRAQ study, appear to correlate better with the

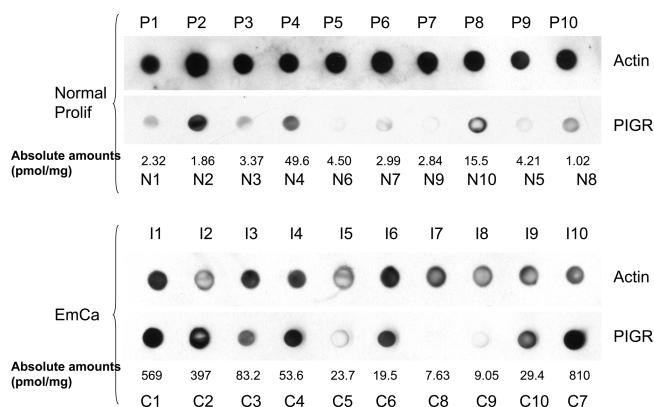


Figure 3. Amounts of PIGR as determined by mTRAQ compared with previous Western dot blot analysis of the same samples. Actin intensities were also included as loading controls. After accounting for differences in loading, intensities of PIGR spots mirror the absolute amounts of PIGR in the samples well. This is evident even among the normal controls where N4 and N10 correspond with the two most intense of the normal proliferative samples in the dot blot. N2 does appear stronger than N4 and N10; however, the actin loading control for N2 shows a much larger amount of total protein was loaded in that well. "P" and "I" were designations used in the discovery phase for normal proliferative and endometrial cancer type I samples; they correspond to the "N" and "C" designations used in this study as shown.

Western analysis than did the originally reported iTRAQ ratios. For example, the highest iTRAQ ratios initially reported among these ten pairs of samples was 5.56 (C2 versus N2);⁵ by contrast, the mTRAQ results suggest that the actual ratio is >200 fold. Similarly, the highest ratio as determined by the mTRAQ result is >800 (C7 versus N8), the iTRAQ ratio for that same pair was reported to be 4.87. Thus, in both these cases, the actual concentration ratios as determined with mTRAQ/MRM were almost 2 orders of magnitude higher than the reported iTRAQ ratios; notably, the Western blot results appear to support the mTRAQ results once the actin loading controls are considered. As mentioned earlier, the first normal proliferative sample in the Western blot is not the same as that used in this absolute quantification experiment. The expression level of this new sample, however, is similar to most of the other normal proliferative samples, and therefore the conclusions drawn should still hold true. This first pair (in the order in Figure 3) shows approximately 2 orders of magnitude higher expression in the cancer sample than that reported by iTRAQ analysis, which was 4.75 fold. Consequently, the results presented here are further proof that, while the iTRAQ ratios correctly reflect the trend in differential expression, their range tends to be compressed, as previously observed.¹⁴

The actual concentrations of both PK and PIGR for both normal and cancer samples were consistent with expectations. PK was determined to be present at an average concentration of 58.33 pmol/mg of total proteins and in the range of 9.13–87.66 pmol/mg in the soluble fraction of the normal proliferative endometrium homogenates (Figure 4A). By contrast, the average concentration of PK in the cancer sample homogenates was 237.2 pmol/mg of total proteins and in the range of 66.10–570.9 pmol/mg. Thus, the average concentration of PK in the 10 cancer samples is approximately 4-fold higher than that of the normal proliferative control samples, and this is consistent with our previous prelimi-

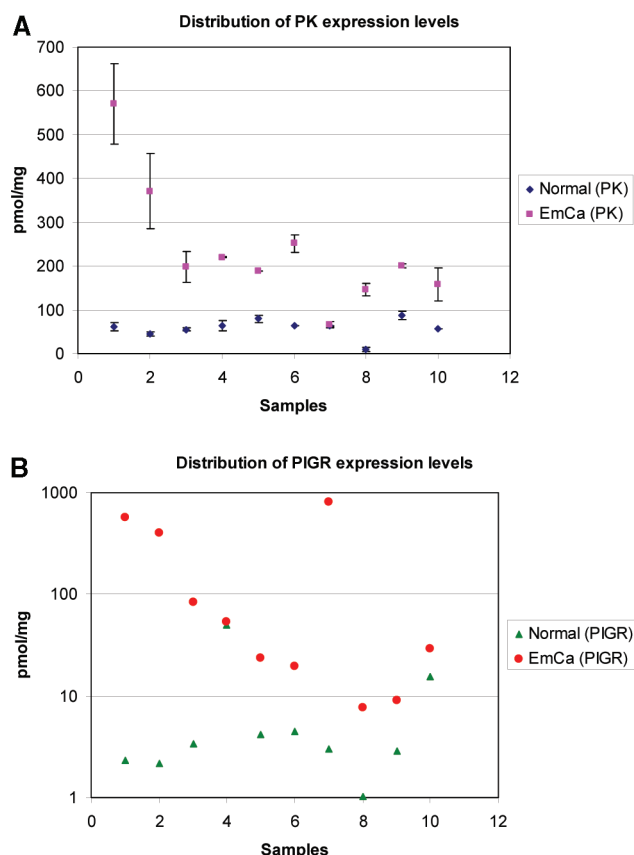


Figure 4. Expression levels of potential biomarkers (A) PK and (B) PIGR in control and cancer samples. Error bars in (A) show ± 1 SD; SD was calculated on the amounts determined using PK1 and PK2 individually. (B) is shown in a semilogarithmic plot to accommodate the range of PIGR expressions.

nary investigation, which had included results obtained by ELISA.¹⁴ The larger variation in expression levels for PK observed in the cancer samples can perhaps be attributed to differences in the proportion of cancerous epithelium within the block of tissue that was homogenized. While it could be argued that the levels of PK detected in the normal proliferative endometrium samples might run counter to expectations as no tumor PK-M2 should be present in the nonmalignant control samples, it is important to note that the analysis performed in this study cannot differentiate between PK-M1 and PK-M2, or for that matter between the dimeric and tetrameric form of PK-M2. As pointed out earlier, PK-M1 and PK-M2 differ by only 22 residues; unfortunately, the tryptic peptide that contains this section, unlike PK1 and PK2, is not consistently detected because of a lower ionization/desorption efficiency.¹⁴ Thus, the PK quantified in the normal proliferative control samples, even if it were PK-M2, might be primarily in the tetrameric form that could be present in the epithelial cells, which in this phase of the normal endometrium are rapidly proliferating. Any investigation into the reason for the presence of PK-M2 would also need to address whether it was present in the dimeric or tetrameric form. The results of the ELISA analysis performed in our preliminary study does strongly suggest that PK-M2 is expressed in the normal endometrium, as the antibody used in that case was specific for the M2 isoform.¹⁴ In light of this, the mTRAQ results from this study appear to provide additional supporting evidence for the presence of the M2 isoform in the

normal proliferative tissue. While the resolution of this question will undoubtedly require further targeted investigation, it is nonetheless interesting to note that the overall expression levels of PK, whether it be in isoform M1 or M2, is markedly different between the two categories of samples.

PIGR was determined to be present at an average concentration of 8.85 pmol/mg of total proteins with a range of 1.02–49.61 pmol/mg in the normal proliferative control samples, and an average concentration of 200.2 pmol/mg with a range of 7.63–810.4 pmol/mg in the cancer samples (Figure 4B). The large variation in expression levels in these samples is consistent with the broad range in expression levels previously reported by the iTRAQ analysis for this protein in these samples. In fact, it was reassuring to note that the exceptionally high amount of PIGR in N4 mirrors our earlier iTRAQ results.⁵ The sample in N4 was labeled as P4 in that study, which had an iTRAQ ratio of 1.96 relative to the average normal proliferative expression for PIGR and was the only outlier among the normal proliferative controls in that study as well. We, therefore, believe that the high expression level reported for PIGR in this sample, as well as the wide range of expression levels among the samples in general, is a consequence of inter-individual variation, and not that of the mTRAQ analysis. Importantly, it should be noted that eight of the ten normal proliferative samples showed PIGR concentrations to be <5 pmol/mg, while all ten cancer samples showed PIGR > 5 pmol/mg, and eight of those >15 pmol/mg. Thus although PIGR does not appear to be as uniformly overexpressed in EmCa relative to the normal proliferative samples, the extent of overexpression, when present, is often orders of magnitude higher than that in the nonmalignant controls.

An advantage in the current, targeted MRM approach using mTRAQ labeling over the earlier, discovery-based approach with iTRAQ labeling is illustrated by the fact that two of the ten cancer samples for which the concentration of PIGR was determined here had previously been missed in the discovery phase. This is consistent with the expectation that MRM provides better certainty of determination than the discovery-based data-dependent analysis. It is also noteworthy that there were almost 3 orders of magnitude differences in the amounts of protein quantified by the MRM method, ranging from approximately 1 pmol/mg of PIGR in N8 to 810 pmol/mg in C7. This is of particular interest, as our iTRAQ analysis on these same samples showed less than 1 order of magnitude differential expression.⁵ This improved dynamic range is a further demonstration of the advantages of the MRM methodology in quantification as practiced on a linear ion-trap tandem mass spectrometer. The differences between the MRM-derived expression values and iTRAQ discovery data could at least partially be attributed to an effect that is sometimes observed in iTRAQ analyses (or any isobaric chemical tagging strategy) in complex mixtures. The selection of a given precursor ion by the first mass analyzer appears to isolate a single peptide, but in complex mixtures there may also be tens to hundreds of other peptides that are both approximately coeluting and approximately isobaric. While these minor peptides are much less abundant than the target peptide and cannot be seen around the precursor ion, the additive effect of hundreds of minor contribution to the iTRAQ reporter ions (m/z 114–117) in the MS/MS spectrum yields a perceptible background. This generic background contribution

to the reporter ions is approximately equal in all four channels, thereby resulting in a biasing of ratios toward unity (i.e., a smaller change in apparent expression ratio). This effect can be attenuated, but not completely removed, by using a higher resolution in the selection of the precursor ion and more extensive fractionation to reduce the complexity of the mixture analyzed at any given time point. By contrast, as MRM measurements are performed using sequence-specific ions, and not common reporter ions, this additive effect is absent and the ratios thus determined are more reflective of the true expression changes. That said, the ability of iTRAQ reagent to discover statistically significant biomarkers is not compromised, as shown by the fact that the differential expressions uncovered during the discovery phase are herewith confirmed by MRM analysis.

It should also be noted that, while the conditions for this particular study were optimized to quantify relatively higher-abundance proteins, the approach itself can be applied to lower-abundance proteins by judicious choice of experimental conditions. These include the use of shallower gradients during fractionation and the injection of larger amounts of the fraction for reverse phase LC-MS/MS. In this study, we performed minimal SCX fractionation and used only one-tenth of the fraction for each subsequent analysis. Obviously, quantifying lower-abundance proteins will require the use of lower concentrations of the peptide quantification standards.

We would also like to emphasize that while this study provided important, qualitative verification of the iTRAQ results, as well as demonstrated the fidelity of MRM and mTRAQ labeling of complex samples, the absolute quantifications in tissue homogenates themselves might not prove to be diagnostically meaningful. This is because the relative amounts of biomarkers are affected by the presence of unrelated and non-cancer cell types within the tissue block. However, this current approach if applied to the quantification of proteins of interest in bodily fluids, including blood plasma, would provide a means to determining the concentrations of such proteins in the normal and diseased populations. In turn, this would ultimately provide a means to establish a threshold concentration in absolute terms, beyond which a test

sample would be deemed to contain biomarker levels indicative of the disease state. A prime example of this is the test for prostate-specific antigen in blood as an aid to the diagnosis of prostate cancer.

CONCLUSION

We have successfully demonstrated that MRM with mTRAQ labeling for biomarker quantification in tissue homogenates is feasible, reproducible, and that the results are complementary to those obtained via differential analysis with iTRAQ labeling, Western blotting, and ELISA. Additionally, the results obtained in this study serve as further verification of the two potential endometrial cancer markers discovered previously, and show that the previous, relatively small ratios indicative of differential expression, particularly in the case of PK, are in fact significantly higher. This establishes the superior performance of targeted MRM analysis on hybrid triple quadrupole/linear ion-trap mass spectrometry over that of discovery analysis on hybrid quadrupole/time-of-flight mass spectrometry for quantification. Planned studies involving similar analyses on bodily fluids will provide data that can eventually serve to aid in disease diagnosis.

ACKNOWLEDGMENT

This research was supported by Canadian Cancer Society Research Grant 06172 of the National Cancer Institute of Canada. Collaboration and support by Applied Biosystems/MDS Analytical Technologies is gratefully acknowledged. We thank Drs. Christie L. Hunter, Sean L. Seymour, and Bruce A. Thomson for helpful discussion.

SUPPORTING INFORMATION AVAILABLE

Individual expression ratios, spectra regarding synthetic peptide purity and details of MRM transitions. This material is available free of charge via the Internet at <http://pubs.acs.org>.

Received for review December 23, 2008. Accepted March 5, 2009.

AC802726A